GeoHealth

RESEARCH ARTICLE

10.1029/2024GH001020

Key Points:

- Daily observations of *Enterococcus* spp. concentrations in a coastal waterway were similar during and outside of perigean spring tides
- Tidal inundation of stormwater networks occurred daily, but rainfall runoff produced the greatest bacterial contamination in the waterway
- High *Enterococcus* spp. concentrations were observed in roadway floodwaters and the receiving waterway during perigean spring tides

Supporting Information:

Supporting Information may be found in the online version of this article.

Correspondence to:

N. G. Nelson,
nnelson4@ncsu.edu

Citation:

Carr, M. M., Gold, A. C., Harris, A., Anarde, K., Hino, M., Sauers, N., et al. (2024). Fecal bacteria contamination of floodwaters and a coastal waterway from tidally-driven stormwater network inundation. *GeoHealth*, *8*, e2024GH001020. https://doi.org/10.1029/2024GH001020

Received 22 JAN 2024
Accepted 27 MAR 2024

Author Contributions:

Conceptualization: M. M. Carr, N. G. Nelson
Data curation: M. M. Carr, N. Sauers, G. Da Silva, C. Gamewell
Formal analysis: M. M. Carr
Funding acquisition: N. G. Nelson
Investigation: M. M. Carr, A. C. Gold
Methodology: M. M. Carr, A. C. Gold, A. Harris, K. Anarde, M. Hino, N. G. Nelson
Project administration: N. G. Nelson
Resources: N. G. Nelson

Fecal Bacteria Contamination of Floodwaters and a Coastal Waterway From Tidally-Driven Stormwater Network Inundation

M. M. Carr[1], A. C. Gold[2], A. Harris[3], K. Anarde[3], M. Hino[4], N. Sauers[1], G. Da Silva[1], C. Gamewell[1], and N. G. Nelson[3,5]

[1]Department of Biological and Agricultural Engineering, North Carolina State University, Raleigh, NC, USA, [2]Environmental Defense Fund, Raleigh, NC, USA, [3]Department of Civil, Construction, and Environmental Engineering, North Carolina State University, Raleigh, NC, USA, [4]Department of City and Regional Planning, University of North Carolina—Chapel Hill, Chapel Hill, NC, USA, [5]Center for Geospatial Analytics, North Carolina State University, Raleigh, NC, USA

Abstract Inundation of coastal stormwater networks by tides is widespread due to sea-level rise (SLR). The water quality risks posed by tidal water rising up through stormwater infrastructure (pipes and catch basins), out onto roadways, and back out to receiving water bodies is poorly understood but may be substantial given that stormwater networks are a known source of fecal contamination. In this study, we (a) documented temporal variation in concentrations of *Enterococcus* spp. (ENT), the fecal indicator bacteria standard for marine waters, in a coastal waterway over a 2-month period and more intensively during two perigean spring tide periods, (b) measured ENT concentrations in roadway floodwaters during tidal floods, and (c) explained variation in ENT concentrations as a function of tidal inundation, antecedent rainfall, and stormwater infrastructure using a pipe network inundation model and robust linear mixed effect models. We find that ENT concentrations in the receiving waterway vary as a function of tidal stage and antecedent rainfall, but also site-specific characteristics of the stormwater network that drains to the waterway. Tidal variables significantly explain measured ENT variance in the waterway, however, runoff drove higher ENT concentrations in the receiving waterway. Samples of floodwaters on roadways during both perigean spring tide events were limited, but all samples exceeded the threshold for safe public use of recreational waters. These results indicate that inundation of stormwater networks by tides could pose public health hazards in receiving water bodies and on roadways, which will likely be exacerbated in the future due to continued SLR.

Plain Language Summary Communities along the US Atlantic Coast have begun to experience the effects of sea-level rise as stormwater drainage pipes, originally designed when sea levels were lower, are now routinely inundated at high tide. We do not know whether frequent inundation of stormwater drainage pipes affects coastal water quality, specifically the fecal bacteria levels of coastal waters. In this study, we collected daily measurements of *Enterococcus* spp. (ENT), the bacteria used by regulators to assess the safety of marine waters for swimmers and recreators, from a tidal creek over a 2-month period. We also collected water samples from roadway floodwaters and the adjacent tidal creek during the highest high tides when the stormwater pipes drained during the outgoing tide. After data collection, we developed statistical models to relate the amount of ENT in the tidal creek to tide, rainfall, and stormwater infrastructure. When comparing rainfall and tide, we observed that rainfall caused greater bacterial contamination in the tidal creek than high tide flooding. However, we observed high ENT concentrations in roadway floodwaters and in the creek during the outgoing tide, leading us to conclude that everyday flooding of underground stormwater pipes at high tide could create hazardous water quality.

1. Introduction

Since 1880, global sea level has risen between 21 and 24 cm due to the melting of land-based ice and thermal expansion of ocean water (Sweet et al., 2022). On the United States' South Atlantic and Gulf coasts, local sea levels have risen at even higher rates (approximately 10 mm year^{-1}) due to internal climate variability (e.g., increased wind-driven ocean circulation) and local land elevation changes (e.g., subsidence and isostatic rebound) (Dangendorf et al., 2023).

Software: M. M. Carr, A. C. Gold
Supervision: N. G. Nelson
Visualization: M. M. Carr
Writing – original draft: M. M. Carr, N. G. Nelson
Writing – review & editing: M. M. Carr, A. C. Gold, A. Harris, K. Anarde, M. Hino, N. Sauers, G. Da Silva, C. Gamewell, N. G. Nelson

This accelerated rate of local or relative sea-level rise (SLR) poses a threat to coastal communities, many which were built on low-lying land. For many of these coastal communities, stormwater infrastructure, like subterranean pipe networks, ditches, and catch basins, was built decades ago when sea levels were lower. Now, increased water levels have allowed tides to propagate into stormwater networks and overtop low elevation land areas, causing coastal communities to flood in what is referred to as "high tide flooding," "sunny day flooding," "chronic flooding," or "nuisance flooding." Regular tidal inundation of stormwater networks has become widespread in coastal areas (Gold et al., 2022), and persistent increases in SLR are projected to increase the frequency and magnitude of high tide flooding nationally (Sweet et al., 2022).

As tidal floods increase in frequency and magnitude, aging and faulty stormwater infrastructure may pose a public health risk by creating water quality hazards (Allen et al., 2019). Stormwater networks can act as reservoirs for fecal contaminants, as exfiltrated sewage (Hart et al., 2020; Olds et al., 2018), biofilms (Burkhart, 2013), or septic leachate (Converse et al., 2011) can be present within the network. Frequent inundation by tidal waters could transport fecal contaminants from stormwater networks to roadways during incoming or flood tides, and flush pollutants into coastal waters during outgoing or ebb tides. Other factors, like stormwater runoff (Gold et al., 2023; Shen et al., 2019) and high groundwater tables (Befus et al., 2023; Habel et al., 2020), can compound with tides and reduce the volume capacity of stormwater networks, leading to more extensive or frequent flooding of coastal communities.

In coastal waters, fecal contamination is often measured by *Enterococcus* spp. (ENT) concentrations. ENT are gram-positive cocci bacteria typically found in the intestines of warm-blooded mammals. Because of their origin in intestines, ENT are used as a fecal indicator organism in marine and beach water quality standards from the U. S. Environmental Protection Agency (EPA, Recreational Water Quality Criteria, 2012). ENT concentration is a proxy measure for gastrointestinal illness risk in marine waters (Wade et al., 2003).

Increased attention has been dedicated to tidal inundation as a transport mechanism of fecal contamination through stormwater infrastructure inundation (Hart et al., 2020; Price et al., 2021), overtopping of coastal infrastructure (Macías-Tapia et al., 2021, 2023), and groundwater inundation (McKenzie et al., 2021). Hart et al. (2020) measured human-specific microbial source tracking markers in a separate storm sewer system in Beaufort, NC, during compound high tide and storm conditions, proposing that diluted sewage could be present in standing water on the roadway when high tide floods occur. This work was continued by Price et al. (2021), who determined that the highest concentrations of fecal indicator bacteria (FIB), including ENT, in stormwater discharge were present in receding tides during 19 sampling events encompassing both storm and ambient conditions. Likewise, Macías-Tapia et al. (2021, 2023) reported consistent exceedances of ENT in tidal floodwaters of the Lafayette River in Norfolk, VA, during five annual perigean spring tide flooding events between 2017 and 2021. Perigean spring tides occur during the coincidence of perigee—when the moon is closest to the Earth in its orbit and therefore exerts a large gravitational pull resulting in higher than average tides—and spring tide (during a new or full moon, when the Earth, moon, and sun are in alignment). Because perigean spring tides produce some of the highest water levels of the year, they can result in coastal flooding of low-lying areas. The work of Macías-Tapia et al. (2021, 2023) determined that in Norfolk, ENT loads varied between perigean spring tide floods but no relationship between ENT abundance and floodwater extent could be determined. Lastly, McKenzie et al. (2021) monitored coastal groundwater, surface water, and storm drain effluent during high tide events in Honolulu, HI, and reported the presence of wastewater discharge in the collected samples through measurement of radon and wastewater tracers. Combined, these studies provide insight into the potential role of tidal flooding as a mechanism for fecal contamination in coastal waters. However, to understand how stormwater network inundation by tides is a driver of coastal fecal contamination, longitudinal data are needed to understand how contaminant dynamics vary across locations, over time, and with flood events of different magnitudes and drivers (e.g., tides and rainfall).

In this study, we assessed the potential for fecal contamination in an urban, coastal waterway that experiences tidal floods and daily inundation of its underground stormwater network by tides. Specifically, our objectives were to (a) document temporal variation in fecal bacteria concentrations in a coastal waterway over multiple flood events and under baseline conditions, (b) measure fecal bacteria concentrations in roadway floodwaters during tidal flood events, and (c) explain variation in bacteria concentrations as a function of tidal inundation, antecedent rainfall, and stormwater infrastructure. Since fecal contaminants are highly variable in space and time (Boehm, 2007), we collected observational data at three locations daily over a 2 month period, and more intensively during 10 tidal cycles coinciding with two perigean spring tide events (i.e., some of the highest tide

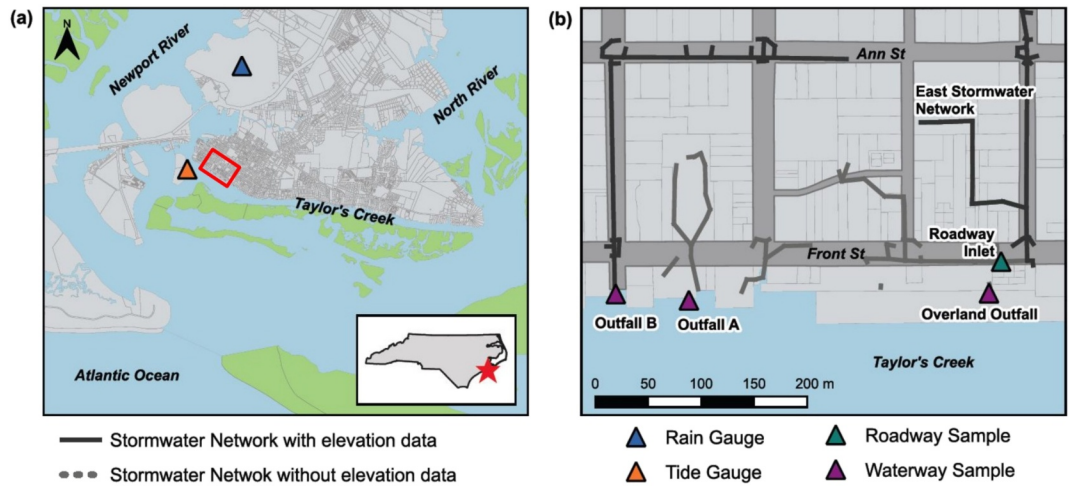

Figure 1. Study map of Beaufort, NC (USA) with an inset map showing the location of Beaufort within North Carolina as a red star (a) and the four stormwater networks in the study area (b). In panel (a), the red rectangle indicates the study area. The green land area represents natural areas, the gray land area represents developed areas, and the thin gray lines delineate land parcels. The NOAA tide gauge (orange triangle), which informed sampling times and provided data for tidal variables, is located across Taylor's Creek approximately 300 m from the Outfall B sampling location. The rain gauge (blue triangle), which provided data for rainfall variables, is located north of the study site. In panel (b), thick gray lines show the underground stormwater pipe network, with the shade of gray indicating whether there was elevation data available (dark and light for networks with known and unknown elevation, respectively). Waterway samples were collected from Taylor's Creek at three locations (purple triangles) within 2 m of stormwater network outfalls. Roadway flood samples were collected directly above a single stormwater catchment grate called the Roadway Inlet (teal triangle) in the East Stormwater network.

events of the year, when the moon is closest to the earth). These measurements, in conjunction with a simplified pipe network model and linear regression, were used to explain variation in bacteria concentrations in the coastal waterway as a function of tidal inundation, antecedent rainfall, and stormwater infrastructure.

2. Methods

2.1. Site Description

Our study site was Beaufort, North Carolina, USA, a small, coastal town established in the 1700s. Beaufort sits on a peninsula between the Newport River and North River (to the west and east, respectively) and north of Taylor's Creek, a tidal channel that empties through an inlet to the Atlantic Ocean. We focused our sampling efforts on Taylor's Creek, which is the receiving water body that is adjacent to the downtown area, and on Front Street, the roadway closest to Taylor's Creek (Figure 1a). The tides in Taylor's Creek are semi-diurnal with a tidal range of 0.95 m (Center for Operational Oceanographic Products and Services, 2022, NOAA Tides and Currents Station ID: 8656483, located in Beaufort, NC). In 2016, Taylor's Creek was listed as a 303(d) impaired waterway for ENT by the North Carolina Division of Environmental Quality, and was later delisted in 2022 after stormwater network improvements (Division of Water Resources, 2023).

Much of the shoreline in the downtown area is armored with bulkheads, which protect roadways and other low-lying land areas from high water levels in Taylor's Creek. Stormwater is conveyed to Taylor's Creek via a separate storm sewer system consisting of subterranean pipes and several outfalls within our sampling area (Figure 1b). Roadway flooding is monitored on Front Street by water level gauges located within the stormwater network, as well as pole-mounted cameras (Gold et al., 2023). These data have shown that tides inundate the stormwater network on a daily basis, and, during perigean spring tide events, water can rise all the way up through the network and result in roadway flooding. During regular tides, flooding can still occur due to the compounding effects of rainfall, as there is limited capacity for pipes to convey rainfall as a result of tidal water volumes occupying some of the capacity (Gold et al., 2023).

Two spring tides coinciding with full moons in perigee on 14 June and 13 July 2022 occurred during the study period (NOAA, 2022). During the 10 highest high tide cycles associated with these perigean spring tide events,

tidal waters propagated up through the stormwater network and produced minor roadway flooding nine times. No concomitant rainfall occurred during the highest high tides of the two perigean spring tide events, so that the floodwaters were produced from tidal influence only. Rainfall occurred during the higher low tide on 15 July 2022, and produced a compound flood event (i.e., rainfall coincided with tidal inundation).

2.2. Data Collection

Water quality samples were collected for enumeration of ENT concentrations, which is a proxy measure for fecal contamination. Collection occurred at three waterway locations in Taylor's Creek (Figure 1b). The "Overland Outfall" sampling location is near a bulkhead spillway that conveys stormwater runoff from a parking lot and is not connected to the subterranean pipe network. The Overland Outfall is relatively high in elevation and was not observed to be inundated during the study period. The "Outfall A" drains a relatively small area (Figure 1b), including a parking lot around a museum and catch basins on Front Street. The "Outfall B" sampling location drains a relatively larger area, including a residential street and catch basins on Front Street and Ann Street (Figure 1b). The Outfall B sampling location was added on 14 June 2022, a week after sampling was initiated at the Overland Outfall and Outfall A locations. Outfall elevations were only available for Outfall B, which is positioned at −0.74 m NAVD88 or −0.30 m Mean Higher-High Water (MHHW). The MHHW datum is the mean of the highest diurnal tide, and is useful for identifying extremes in tidal heights. Water levels greater than the 0 m MHHW datum are deviations of tidal heights above the average high tide. At this elevation, Outfall B is inundated by tides on a daily basis.

Collection of water samples in Taylor's Creek, proximate to the three outfall locations described above, occurred daily for 58 days from 6 June to 2 August 2022. This allowed for characterization of fecal contamination during both baseline and perigean spring tide conditions. Baseline sampling of ENT occurred daily between 8:00 and 9:00 a.m. Eastern Standard Time to prevent ENT levels from being affected by UV inactivation from direct sunlight, which peaks around midday. Given the 2 month long sampling period, the daily samples also captured every tidal stage (i.e., low, rising, high, and falling tide stages). Perigean spring tide sampling of ENT occurred on 12–16 June and 11–15 July 2022, when estimated water levels were above the local risk-based flooding threshold. During these high water level events, we increased the sampling frequency to include measurements at the higher high tide, ebb tide (approximately halfway between high and low tide), and low tide, with measurement times scheduled based on predicted water levels at the nearby NOAA Tides and Currents Station (ID 8656483; Figure 1). This sampling frequency was selected to capture the change in fecal contamination conditions from the maximum stormwater inundation (at the higher high tide) and during the draining of the stormwater networks (during the ebb tide and at the higher low tide). During these perigean spring tide events, we also sampled roadway floodwaters at a stormwater catchment grate (Roadway Inlet) in the easternmost stormwater network of the downtown area, referred to as the "East" network ($n = 10$). We define a roadway flood as any amount of water above the elevation of the stormwater catchment grate. In total, 166 samples were collected from Taylor's Creek under baseline conditions (58 at Overland Outfall and Outfall A, 50 at Outfall B) and 89 during perigean spring tide events (30 at Overland Outfall and Outfall A and 29 at Outfall B, corresponding to three measurements per studied tidal cycle, with five cycles measured during each of the two perigean spring tide periods). Additionally, 10 samples were collected from roadway floodwaters (9 tidal floods, 1 compound flood).

Sterile, pre-rinsed 100 mL FalconTubes (polypropylene material) attached to a sampling pole were used to collect 100 mL water samples from Taylor's Creek at 0.5–1 m below the water surface at the three waterway locations, which were within 2 m of stormwater network outfalls. For flood water samples collected at the stormwater catchment grate, collection occurred by hand at water surface depth. After collection, samples were stored in a cooler at 4°C during transport to the laboratory. Water samples were processed in duplicate for ENT following the IDEXX Enterolert standard protocol with the Quanti-tray 2000 (IDEXX, 2019). The IDEXX assay requires a 100 mL sample volume. Per the IDEXX Enterolert protocol, due to the brackish salinities of the water samples, 10 mL of water sample was mixed with 90 mL of deionized water during processing. Samples were provided the IDEXX media and incubated for 24 hr at 41°C ± 0.5°C. ENT concentrations were enumerated using a most-probable number (MPN) technique based on the number of large and small wells of the quanti-trays fluorescing under UV light, with a modified laboratory detection range of 10–24,196 MPN ENT per 100 mL water (MPN 100 mL^{-1}) due to sample dilution. During sample collection and laboratory analysis, field blanks ($n = 27$) and laboratory blanks ($n = 30$) were collected and processed for quality assurance and quality control purposes. Field blanks consisted of deionized water in sample bottles that were transported to and from the field in a sample

cooler, and opened and recapped at one or more of the sampling sites. Lab blanks consisted of deionized water in sample bottles that remained in the lab and were not transported to the field.

ENT concentrations were classified as above or below the EPA's single sample maximum threshold concentration for safe public use of recreational waters of 104 MPN 100 mL^{-1} (EPA, Recreational Water Quality Criteria, 2012). This EPA standard is for recreational use of marine waters, meaning it directly applies to water samples collected from Taylor's Creek but does not directly apply to roadway floodwaters, which are not recreational waters. Given that a standard does not exist for floodwaters of any kind, whether storm or tidally driven, but pedestrians can still make contact with floodwaters, we consider the EPA's recreational standard as a benchmark for comparison of water quality measurements collected from the roadway during the tidal floods.

2.3. Pipe Network Inundation Model

A pipe network inundation model of Front Street was used to characterize the extent of tidal inundation within the stormwater network during the measured flood events. Generally, a pipe network inundation model is a "bathtub" approach that simulates flooding by gradually filling subterranean pipes based on the elevation of the pipe relative to tidal stage (Strauss et al., 2012). The pipe network inundation model used in this study was generated using the *bathtub* R package (Gold et al., 2022) and is the same model used by Gold et al. (2022) for Beaufort, NC. This model was developed using elevations from a 2017 survey, which was conducted when some stormwater structures were inaccessible. Hence, our pipe network inundation model is incomplete for the Front Street study area, but can be used to estimate stormwater network inundation in two of the studied stormwater pipe systems, specifically the pipe networks of the Outfall B and Roadway Inlet (located in the East network) sampling locations (Figure 1b). The percentage of stormwater network inundation was quantified at discrete water levels by averaging the percent fill of surveyed stormwater point structures (e.g., drop inlets and catch basins) on Front Street and Ann Street.

2.4. Explanatory Variables Used in Linear Regressions

We sought to explain measured variation in ENT concentrations within the waterway with both tidal and rainfall factors using robust linear mixed effect regressions of the baseline sampling and the perigean spring tide sampling data. Tidal variables used in the explanatory analysis include tidal height at time of sample collection, time since the last high tide before sample collection, and the height of the last high tide before sample collection. Tidal height at the time of sample collection was taken from the nearby NOAA Tides and Currents gauge (Figure 1a), which has been shown to match well with measured water levels in a stormwater catch basin on Front Street when it is not raining (Gold et al., 2023). The height of the last high tide, and the time since the last high tide, were likewise calculated using the NOAA tide gauge data. We include time since the last high tide before sample collection and the height of the last high tide before sample collection to account for a potential lagged response of ENT concentrations in the waterway as tidal waters recede from the stormwater network, relative to the timing of maximum inundation of the stormwater network. While additional meteorological observations are available at the NOAA tide gauge, such as air temperature, we chose to only focus on the effects of tide and rain given our study period spanned two summer months and, thus, was not long enough to account for the effects of seasonal variation.

Because Taylor's Creek is a coastal waterway, it receives ENT loads by both direct runoff from stormwater outfalls and fluvial transport through the local watershed. To account for these transport pathways, we considered multiple cumulative rainfall factors in the explanatory analysis. Seven rainfall variables were analyzed, all of which correspond to antecedent rainfall totals over finite intervals, including rainfall over 3, 6, 12, 24, 36, 48, and 72 hr prior to sample collection (in mm). These variables were calculated using hourly rainfall depths (mm) obtained from the Michael J. Smith Airport weather station located approximately a mile north of Front Street in Beaufort, NC (North Carolina State Climate Office of North Carolina, 2022, station ID: KMRH; Figure 1a). The June rainfall total was 50 mm, and only one storm event produced a rainfall depth over 13 mm (or 0.51 inches). In contrast, the July rainfall total was 400 mm, and 8 storm events produced rainfall depths greater than 13 mm.

2.5. Regression Analysis

Prior to regression analysis, ENT concentrations from the waterway were logarithmically transformed to account for the exponential range of bacteria counts observed. The relationship between logarithmically transformed ENT

concentrations ($\log_{10}$ ENT) and sampling location was assessed using the Friedman test, which is a hypothesis test for repeated measures. We selected the Friedman test because the daily collection of ENT constitutes a repeated measure and the Friedman test does not assume an underlying distribution for the grouped-by-location data. The Friedman test determines whether the median value of a treatment group is significantly different from the median values of the other treatment groups. We assessed significance with an alpha value of 0.05. The Friedman test was calculated using the *stats* R package (R Core Team, 2013).

Next, the relationships between $\log_{10}$ ENT, tidal, and rainfall variables were analyzed using two sets of robust linear mixed effect models with the *robustlmm* R package (Koller, 2016). We selected robust linear mixed effect models because of the repeated-measures structure of our sampling design and the presence of outliers and non-normal residuals in the $\log_{10}$ ENT data set. The first set of models (the "baseline" models) used data from the entire 2-month study period, which captured daily stormwater network inundation and multiple rain events. The second set of models (the "perigean spring tide" models) used data from the perigean spring tide sampling on 12–16 June and 11–15 July 2022. Data collected during baseline sampling and perigean spring tide sampling were modeled separately due to differences in sampling design and to allow for assessment of relationships between tide and rainfall variables under distinct conditions. The model sets were comprised of individual robust linear mixed effect regressions between $\log_{10}$ ENT and a single explanatory variable to evaluate pairwise relationships.

Given that the waterway data varies both in space and time, the baseline mixed effect model has the following equation structure:

$$\log_{10}\ \text{ENT} = \text{Explanatory Variable} + (1|\text{Site}) \quad (1)$$

where "|" denotes that the sampling location, or "Site" (Overland Outfall, Outfall A, or Outfall B), is a random effect. The perigean spring tide model has the equation structure:

$$\log_{10}\ \text{ENT} = \text{Explanatory Variable} + (1|\text{Site}) + (1|\text{Perigean Spring Tide/Categorical Tidal Stage}) \quad (2)$$

where "Site" and "Perigean Spring Tide" (June or July) are random effects and "Categorical Tidal Stage" (high, ebb, and low tide) is a nested random effect within the "Perigean Spring Tide" random effect denoted by "/". No interaction exists between the "Site" and "Perigean Spring Tide/Categorical Tidal Stage" terms because the sampling design produced a crossed-data structure between sampling period and site. The tidal and rainfall explanatory variables are fixed effects and were centered and scaled in the baseline models and perigean spring tide models. Conditional R^2 (variance explained by random and fixed effects) and marginal R^2 (variance explained by fixed effects or explanatory variables only) were calculated for each regression using the *performance* R package (Lüdecke et al., 2021). Results are discussed in terms of their marginal R^2 value since marginal R^2 values only include the effect of the explanatory variable while conditional R^2 values also include the effects of random variables. Additionally, p-values and slopes were calculated to identify significant positive or negative relationships (alpha = 0.05) using the *parameters* R package (Lüdecke et al., 2020). All analyses were performed using R version 4.2.2 (R Core Team, 2022).

3. Results and Discussion

3.1. Tidal Stormwater Network Inundation Occurred Daily

Water level data from within a storm drain on Front Street showed that the East network was inundated daily over the 2 month study period at the higher high tide ($n = 58$, Gold et al., 2023). Using the pipe network model, we find that the stormwater network along other areas of Front Street was inundated 57% at the average higher high tide height of 0.16 m MHHW and inundated 0.6% at the average lower low tide height of −0.91 m MHHW during baseline conditions (Figures 2a and 2b). During the perigean spring tide events, the average lower low tide and higher high tide elevations were −1.1 and 0.40 m MHHW, respectively, which correspond to modeled stormwater network inundation percentages of 0% and 78% along Front Street, respectively (Figures 2c and 2d). During the perigean spring tide events, inundation of the stormwater network extended inland beyond Front Street, filling pipes nearly 40% with tidal water (Figure 2c).

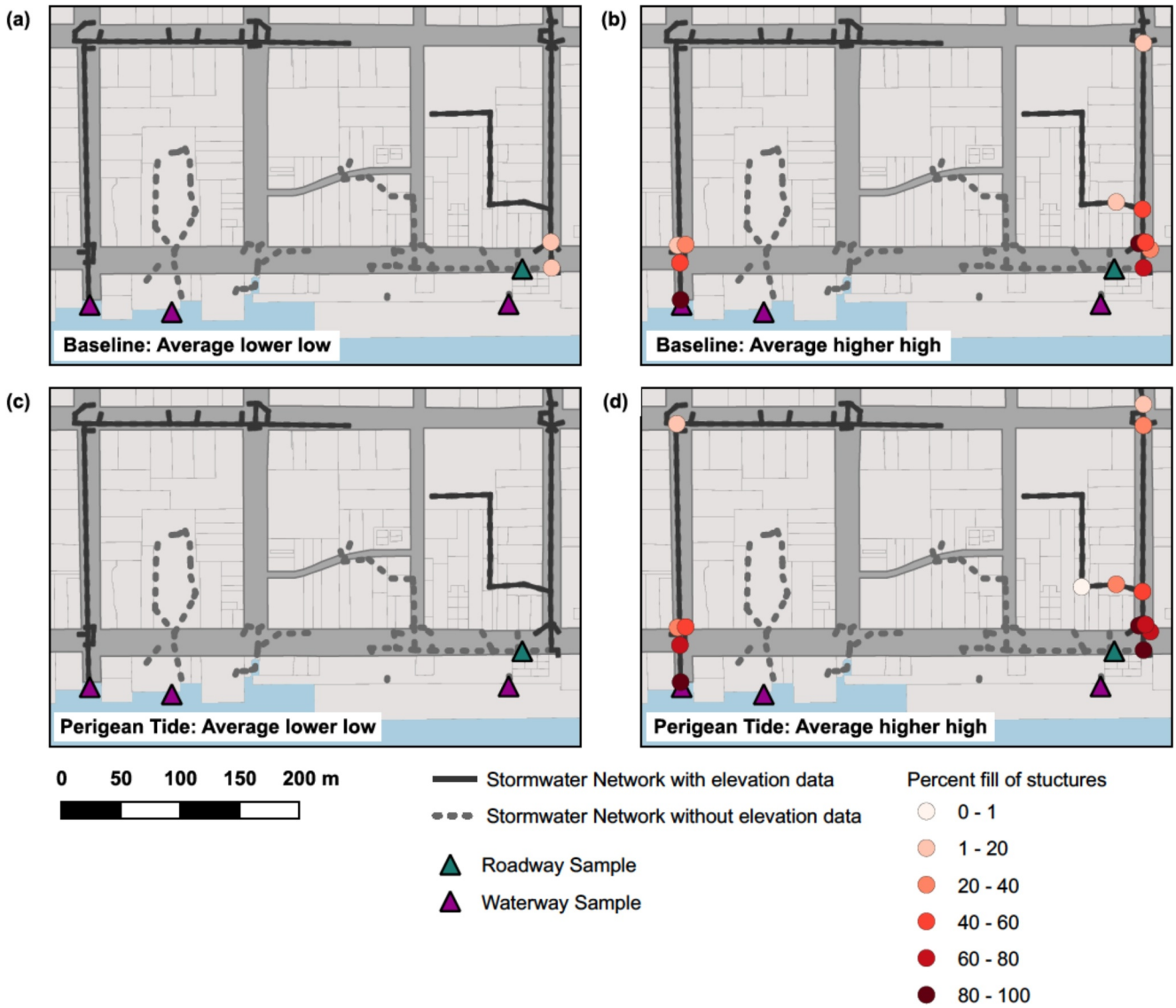

Figure 2. Modeled tidal inundation of two stormwater networks in downtown Beaufort during the study period. The average percent fill of stormwater catchments (attached to subterranean pipes) is shown for lower low tide (a, c) and higher high tide (b, d) for the baseline data collected from 6 June to 2 August 2022 (a, b), and for the perigean spring tide data collected on 12–17 June and 11–16 July 2022 (c, d).

Our pipe network model only accounts for variation in tidal elevation, as measured by the nearby NOAA tide gauge, and does not consider water level contributions from rainfall runoff, groundwater infiltration into the stormwater network, or pipe hydraulics. Bathtub models, like the pipe network model used here, typically overestimate flooding compared to models that account for pipe hydraulics (e.g., Castrucci & Tahvildari, 2018; Gallien et al., 2014). However, outside of rain events, Gold et al. (2023) showed that water levels in the East network track well with water levels measured at the NOAA tides gauge during baseline conditions, indicating that contributions from groundwater infiltration into the stormwater network are likely small for the pipe network. During rainfall events, the pipe network model is an underestimate of actual inundation.

While the network inundation model does not consider non-tidal forcings and pipe hydraulics, it can be used to estimate where inundation was relatively high and low across the network due to tidal forcing alone. In particular, the network inundation estimates highlight that total network inundation and roadway flooding were most likely to occur in and along the East network. The pipe network model also reveals that the Outfall B network experienced daily and major inundation, but to a lesser extent than the East network. Due to the inlet and outfall

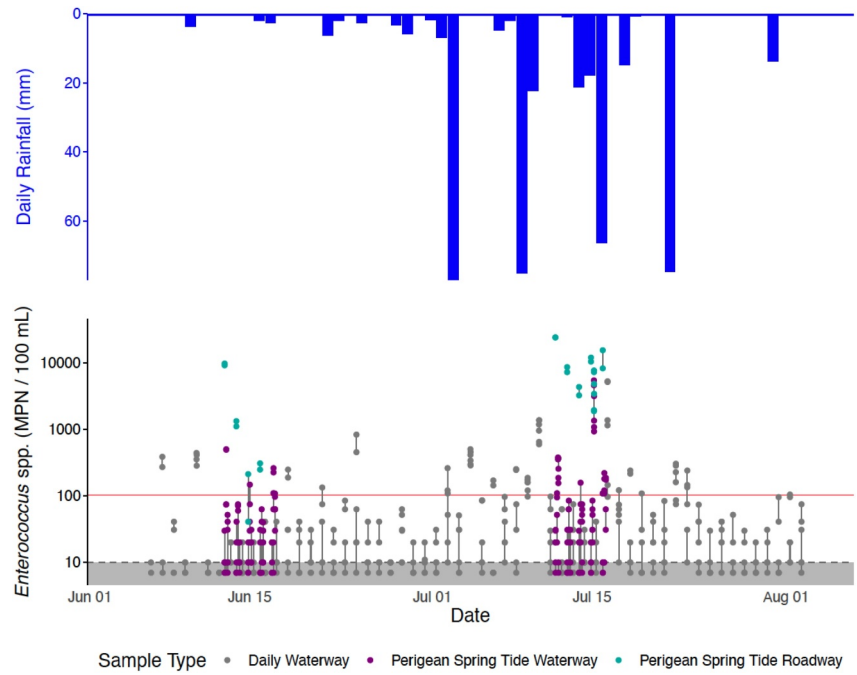

Figure 3. Daily rainfall (top) and *Enterococcus* spp. (ENT) concentrations (bottom) during baseline and perigean spring tide conditions throughout 6 June to 2 August 2022. ENT concentrations are plotted on a $\log_{10}$ scale. The red line represents the EPA's single sample maximum threshold concentration for safe public use (104 most-probable number (MPN) 100 mL^{-1}), and the grayed area represents the minimum detection limit range (below 10 MPN 100 mL^{-1} for samples diluted 10:1). Gray and purple points correspond to measurements taken in Taylor's Creek during baseline and perigean spring tide conditions at the three sampling locations, respectively, while teal points correspond to measurements taken from roadway floodwaters above a single stormwater catchment grate in the East network. Samples were processed in duplicate, and duplicate measurements are connected by vertical lines to visualize uncertainty.

elevations not being surveyed, we are unable to assess the frequency at which the Outfall A network was inundated.

3.2. Daily Waterway ENT Concentrations Differed Between Sampling Locations

ENT was detected in 73% of the daily, or baseline, samples ($n = 241/330$) with concentrations ranging from 10 to 5,298 MPN 100 mL^{-1} (Figure 3). ENT measurements exceeded the single sample maximum threshold concentration for safe public use of recreational waters (104 MPN 100 mL^{-1}) in 16% of the daily samples, indicating recurring but infrequent levels of unsafe fecal contamination in the waterway during the 2 month summer sampling period. Similar daily ENT concentrations in the waterway were observed between non-perigean and perigean spring tide periods. Hence, while perigean spring tide events lead to increased stormwater network inundation (Figure 2d), they did not necessarily result in increased ENT loading within the waterway.

We also found there were significant differences in ENT concentrations by sampling location (p-value = 0.004, Table S1 in Supporting Information S1). During baseline conditions, Outfall B had the highest median concentration of ENT in the waterway (31 MPN 100 mL^{-1}) while the sampling locations Outfall A and Overland Outfall showed lower median ENT concentrations of 10 MPN 100 mL^{-1}, which corresponds to the minimum detection limit. Inter-site variability between outfall sampling locations was also noted by Price et al. (2021), who posited that site-specific infrastructure can cause localized water quality dynamics. However, while significant differences were observed across the three sampling locations, the median concentrations demonstrate how ENT levels were frequently low and well below the EPA recreational water quality standard.

In addition to varying by location, the median ENT concentrations across the outfall locations differed between the months of June and July 2022 (Figure 3, Table S2 in Supporting Information S1). For June, the median ENT concentration was 20 MPN 100 mL^{-1} and had an interquartile range of <10 to 23 MPN 100 mL^{-1} while the July median concentration was 41 MPN 100 mL^{-1} and had an interquartile range of 10–86 MPN 100 mL^{-1}. Rainfall

occurred more frequently in July than in June. Periods of increased rainfall are known to correspond with increased FIB concentrations in coastal waterways due to runoff-driven contamination and elevated surficial groundwater elevations, which can also lead to greater sewage exfiltration (Sercu et al., 2011).

3.3. Roadway Floodwaters Had Consistently High ENT Concentrations

During perigean spring tide events, we visually observed nine minor high tide floods localized to the East stormwater network, and no roadway flooding above the Outfall A and Outfall B stormwater networks. The presence of flooding was corroborated by the storm drain water level measurements and the pipe network model. The floodwater samples exceeded the EPA's single sample maximum threshold concentration for safe public use (104 MPN 100 mL^{-1}) for 8 of the 9 high tide flood events, in many cases by an order of magnitude (Figure 3). These ENT concentrations are comparable to the concentrations reported by Macías-Tapia et al. (2021) in Norfolk, VA in 2017, when 95% of the ENT samples exceeded the single sample maximum threshold concentration and ENT concentrations ranged from 30 to >24,000 MPN 100 mL^{-1}.

In the June perigean spring tide event, the median floodwater concentration was 710 MPN 100 mL^{-1} and concentrations ranged from 41 to 9,804 MPN 100 mL^{-1} (Figure 3). In comparison, in July, the median floodwater concentration was 9,563 MPN 100 mL^{-1} and concentrations ranged from 1,882 to >24,196 MPN 100 mL^{-1}. The perigean high tide elevations were similar between June and July (0.35–0.51 and 0.34–0.45 m MHHW, respectively), as was the modeled inundation percentages at higher high tide (75%–87% and 73%–81%), so we hypothesize that differences in concentrations stem from antecedent rainfall factors. These findings suggest that antecedent rainfall can enhance fecal contamination in roadway floodwaters during high tide flood events. But, importantly, given that the June floodwaters were still more than six times higher than the EPA standard in the absence of antecedent rainfall, complete inundation of stormwater networks by tides in drier conditions can create concerning water quality conditions in roadway floodwaters.

The sources of fecal bacteria in the roadway floodwater samples are unknown, though we believe the primary fecal bacteria sources during the high tide floods sampled were within the stormwater network. We observed fecal contamination in roadway floodwaters in the absence of rain, due solely to stormwater network inundation by tides, indicating a source from either Taylor's Creek or the stormwater network. However, because water quality samples collected near stormwater outfalls in Taylor's Creek did not have similarly high concentrations (Figure 3), Taylor's Creek is likely not a primary source of fecal bacteria to the floodwaters. Lastly, the majority of the roadway floods were small and confined to puddles around the storm drains (Figure 4), indicating that the floodwaters likely did not flush fecal matter from the land surface.

Because tidal inundation of stormwater networks can impede drainage of stormwater runoff, stormwater runoff with high ENT concentrations may remain in the network as stagnant water for extended periods of time, potentially spilling onto the roadway during the next high water level event. Additional sources of fecal bacteria in the stormwater network could include exfiltrated sewage (Hart et al., 2020) or environmental reservoirs of bacteria in biofilms and sediment (Burkhart, 2013). Importantly, since the majority of our measurements were collected from roadway floods with small overland extents, we are unable to assess whether high ENT concentrations would persist during more extensive floods, or if more extensive floods may dilute ENT concentrations instead, as proposed by Lewis et al. (2013).

3.4. Highest Median ENT Concentrations Occurred During Ebb Tide

To capture the water quality of receding tidal waters from the stormwater network during the perigean spring tide events, ENT measurements were collected at multiple tidal stages in the waterway: at higher high tide, ebb tide, and higher low tide (Figure 5). We observed a general trend that ENT concentrations increased from the higher high tide to ebb tide and decreased from ebb tide to the higher low tide. This trend has been previously reported for Taylor's Creek in Price et al. (2021), who observed that ENT increased during ebb tide as tidal height decreased and the stormwater network drained. In this present study, median concentrations at high, ebb, and low tide across the June and July perigean spring tide events were 10, 52, and 30.5 MPN 100 mL^{-1}, respectively (Figure 5). Sixty percent ($n = 36/60$) of high tide samples had ENT concentrations below the minimum detection limit of 10 MPN 100 mL^{-1}. Then, as the tidal waters receded from the stormwater network during ebb tide, ENT concentrations increased, with exceedances of the EPA recreational water quality standard primarily occurring on ebb tide. From the linear regression analysis of the perigean spring tide models, we found that this trend was reflected in a

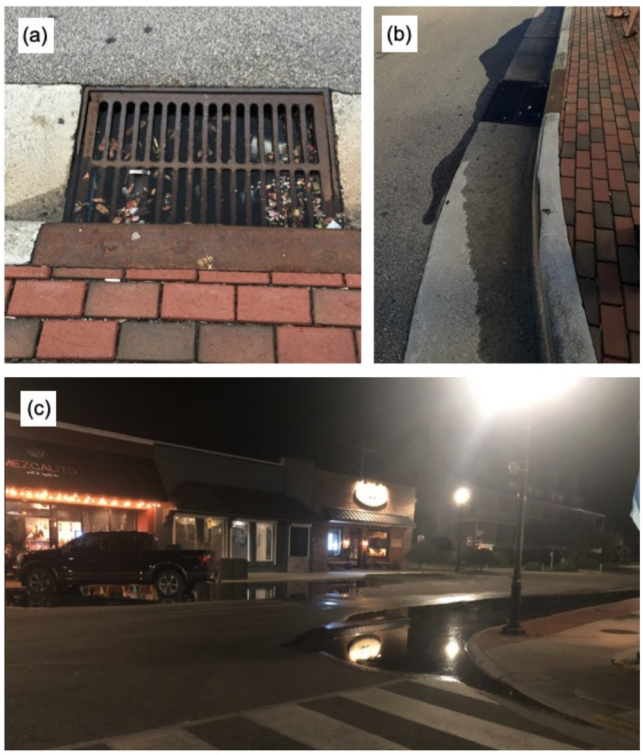

Figure 4. Tidal flooding at high tide on 12 June 2022 at 7:18 p.m. (a), 14 June 2022 at 8:52 p.m. (b), and 15 June 2022 at 9:51 p.m. (c). We define a roadway flood as any amount of water above the elevation of the stormwater catchment grate.

significant negative relationship (coefficient = −0.28, p-value < 0.001) between tidal stage at sample collection and ENT concentrations (Table 1). This increase in median ENT concentrations from high to ebb tide suggests that receding tides transport ENT from the stormwater network to the waterway. However, we also observe a decrease in median ENT concentrations from ebb to low tide, which suggests that the effect of receded tidal waters on ENT concentrations in the waterway was short lived. This could potentially be explained by flushing or dilution. UV inactivation should not have affected the measured ENT concentrations given that the perigean spring tide sampling occurred at night during the June and July events. While most of the EPA recreational water quality standard exceedances occurred from samples collected during ebb tide, a few exceedances were observed outside of ebb tide during the last monitored tidal cycle, which occurred following rainfall (Figure 5b).

Although the highest ENT concentrations in the waterway during the perigean spring tide events were observed during ebb and low tide, the majority of concentrations were below the EPA's threshold for safe public use, demonstrating that the observed conditions did not pose a public health hazard. Yet, the observed increase in ENT concentrations during ebb tide in a large and dynamic waterway like Taylor's Creek demonstrates that tidal floods and stormwater network inundation can serve as a source of fecal contamination to surface waters and are worthy of further investigation as an emerging public health concern, particularly in coastal communities that drain to relatively small tidal creeks with minimal potential to flush or dilute pollutants.

From the results of the robust linear mixed effect models for the perigean spring tides (Table 1), tidal height at sample collection and time to last high

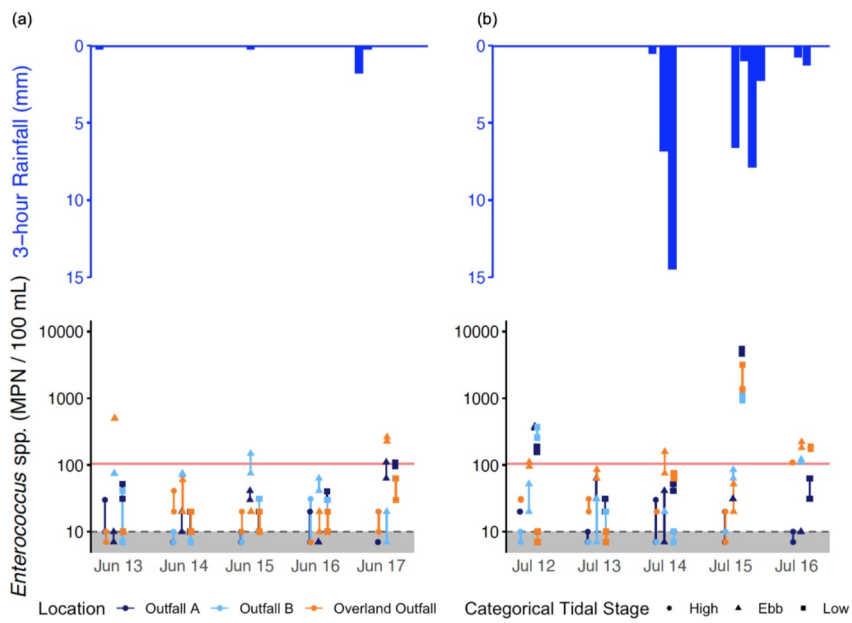

Figure 5. 3-hour rainfall (top) and *Enterococcus* spp. concentrations (bottom) from Taylor's Creek during perigean spring tide events from 12–17 June 2022 (a) and 11–16 July 2022 (b). The red line represents the EPA's single sample maximum threshold concentration for safe public use (104 most-probable number (MPN) 100 mL^{-1}), and the grayed area represents the minimum detection limit (below 10 MPN 100 mL^{-1} for samples diluted 10:1). Point shapes correspond to the tidal stages of high, ebb, and low, while the colors correspond to sampling locations.

Table 1
Linear Regression Models of Baseline Conditions (Top) and Perigean Spring Tide Conditions (Bottom) Between log_{10}-Transformed Enterococcus spp. Concentrations (log_{10} Most-Probable Number) and Tidal or Rainfall Factors

Explanatory variables (fixed effect)	Conditional R^2 (full model)	Marginal R^2 (fixed effects)	p-value (alpha)	Coefficient	Standard error
Baseline conditions (n = 166 observations); random effect = sampling location					
Tidal factors					
Tidal height	0.174	0.056	<0.001	−0.15	0.03
Time to last high tide	0.159	0.037	<0.001	0.12	0.03
Height of last high tide	0.124	0.009	0.073	−0.06	0.03
Rainfall factors					
Prior 3-hr rainfall	0.231	0.105	<0.001	0.21	0.03
Prior 6-hr rainfall	0.273	0.144	<0.001	0.24	0.03
Prior 12-hr rainfall	0.385	0.268	<0.001	0.34	0.03
Prior 24-hr rainfall	0.458	0.346	<0.001	0.38	0.03
Prior 48-hr rainfall	0.395	0.313	<0.001	0.36	0.03
Prior 72-hr rainfall	0.301	0.212	<0.001	0.29	0.03
Perigean spring tide conditions (n = 89); random effects = sampling location, categorical tidal stage, perigean spring tide					
Tidal factors					
Tidal height	0.34	0.206	<0.001	−0.28	0.07
Time to last high tide	0.348	0.134	0.041	0.22	0.11
Height of last high tide	0.394	0.006	0.212	−0.05	0.04
Rainfall factors					
Prior 3-hr rainfall	0.415	0	0.775	−0.01	0.05
Prior 6-hr rainfall	0.373	0.003	0.516	0.03	0.05
Prior 12-hr rainfall	0.376	0.002	0.558	0.03	0.05

tide were associated with the greatest and second greatest marginal R^2 values (0.21 and 0.13, respectively). Though they cannot explain the majority of ENT variance (i.e., they do not have marginal $R^2 > 0.5$), the marginal R^2 values of tidal height at sample collection and time to last high tide support prior recommendations by Price et al. (2021) that tidal variables be included and documented as part of coastal ENT monitoring efforts, as tidal effects can play a role in transporting ENT within coastal systems.

For the perigean spring tide models, height of the last high tide and rainfall variables had low marginal R^2 values and coefficients that were not significantly different from zero (Table 1). Because height of last high tide was not a significant descriptor of ENT concentration variance, we conclude that maximum inundation prior to sampling was not the most important factor explaining the elevated ENT concentrations during ebb tide. Regardless, height of the last high tide should not be discounted as a potential variable to monitor, as our observational period may not have captured high enough water level events to exhibit a significant relationship with ENT concentration. Future SLR projections indicate more frequent and greater inundation of stormwater networks, such that height of the last high tide may become an important factor to explain elevated ENT concentrations as tidal water could reach sources of fecal contamination further into the stormwater network. Additionally, since data collection occurred in one municipality, other coastal stormwater network configurations may have increases in ENT concentrations at tidal heights comparable to the tidal heights measured in this study.

Likewise, our results should not indicate that rainfall is not an important descriptor to ENT variability during the ebb tide and drainage of the stormwater network, as other studies have demonstrated a direct link between rainfall and ENT concentration in coastal waterways (Mallin et al., 2000). The low marginal R^2 values of our tested rainfall variables likely stem from our sampling design, which targeted the tidal dynamics of the 6–7 hr period between the higher high tide and the higher low tide, and did not include many rainfall events.

3.5. Stormwater Runoff Drives Higher ENT Concentrations Than Tidal Inundation

During baseline conditions, stormwater runoff drove higher ENT concentrations in the waterway than tidal inundation. Prior rainfall totals were significantly related to daily ENT variance in the waterway during baseline conditions (Table 1). Specifically, antecedent rainfall over 3, 6, 12, 24, 48, and 72 hr prior to sample collection had larger marginal R^2 values (0.10–0.35) in the baseline model than the significant tidal variables (0.04–0.06). The marginal R^2 values were greatest for the 24-hr ($R^2 = 0.346$) and 48-hr rainfall models ($R^2 = 0.313$), likely demonstrating the lagged effect between rainfall and the accumulation of runoff over the broader watershed drainage area. Many studies have reported increased FIB concentrations in waterways following rainfall events (Converse et al., 2011; Gonzalez et al., 2012; Parker et al., 2010; Stumpf et al., 2010). However, while antecedent rainfall predominantly explained ENT concentrations during baseline conditions (i.e., when there is no roadway flooding from complete stormwater inundation by tides), rain variables did not significantly explain ENT variance during perigean spring tides, as discussed above.

Though rain variables were not significant descriptors of ENT variance during perigean spring tides, we observed that rainfall coincided with the maximum ENT concentrations observed in Taylor's Creek during the perigean spring tide sampling window (Figure 5). On 15 July 2022, sample collection of the low tide samples coincided with a compound flood that was caused by rainfall plus reduced capacity in the stormwater network due to tidal inundation. These samples were collected 20 hr after a 22-mm, 8-hr rainfall event that occurred the previous day, and during the first hour of a 17-mm rainstorm that lasted over 9 hr. Approximately 3.6 mm of rainfall occurred during the first hour of the event. This compound flood event had the greatest ENT concentrations observed in the waterway during both perigean spring tide events, indicating that compound flood events have the potential to bring greater magnitudes of fecal contamination to waterways compared to tidal inundation alone. Further research is needed to quantify the relationship between rainfall depth, extent of tidal inundation, and the magnitude of fecal contamination in the waterway, however our sampling of this one compound flood event demonstrates the importance of how different flood types can cause varying amounts of fecal contamination in coastal waterways.

4. Conclusions

Our findings indicate that chronic stormwater network inundation and tidal flooding caused by SLR present pathways for fecal contamination of coastal surface waters, but research is needed to fully understand whether network inundation and floods create public health hazards. In this study, we consistently observed high ENT concentrations above the US EPA's single sample maximum threshold for safe public use of recreational waters in tidal floodwaters on a roadway in Beaufort, NC, but did not observe similarly concerning ENT concentrations in Taylor's Creek, the adjacent coastal waterway, from tide-driven stormwater network inundation. We observed minor floods with minimal overland footprints, leading us to believe that the sources of the elevated ENT in the floodwaters were within the stormwater network, and could include undrained stormwater runoff, pipe biofilms and sediment, and exfiltrated sewage. Rainfall-driven runoff produced higher ENT concentrations in Taylor's Creek than stormwater network inundation and tidal flooding, reinforcing that stormwater runoff is the dominant driver of increased ENT concentrations in the coastal waterway at present. However, we observed short-lived increases in ENT concentrations in Taylor's Creek as perigean spring tides receded from the stormwater network, and we hypothesize the temporary increase in ENT concentrations is due to dilution or flushing given that Taylor's Creek is a large coastal waterway. In relatively small tidal creeks draining urban centers, the effects of dilution and flushing may not be as apparent, and the role of stormwater network inundation and tidal flooding on ENT concentrations may be more pronounced.

This study provides needed longitudinal water quality observations across a 2-month period that included nine tidal floods from two perigean spring tide events. The longitudinal data allowed us to assess potential public health hazards from tidal flooding and make inferences on the relative roles of stormwater network inundation, tidal flooding, and rain on fecal contamination both in a coastal waterway and roadway floodwaters. However, the small size of the tidal floods we observed prevents us from concluding whether more extensive floods are associated with higher or lower ENT concentrations. Additionally, while our results demonstrate that tidal floods are associated with the problematic water quality impacts shown in previous studies (Hart et al., 2020; Macías-Tapia et al., 2021, 2023; McKenzie et al., 2021; Price et al., 2021), similar studies as the one presented here should be conducted across more locations to better define the site-specific effects related to stormwater infrastructure

and land use. We suggest that future work incorporate sampling across multiple seasons, communities, and flood extents to better understand the prevalence of poor water quality from chronic stormwater network inundation and tidal flooding. Seasonal differences may contribute to the persistence of ENT within the stormwater network, while community differences in infrastructure, topography, land use, and waterway size could contribute to the type and number of ENT sources as well as the effect of tidal flushing on ENT concentrations in the waterway.

Ultimately, the water quality effects of chronic stormwater network inundation and tidal flooding are evolving given the non-stationarity of global climate change and SLR. SLR brings uncertainty to whether tidally-driven inundation and associated pollutant loading will remain at their current levels, as the magnitude of the loading will likely change with increased flooding frequency and damage to infrastructure. For Beaufort and other cities on the Atlantic coast of the US, rates of SLR are 30% higher than the global average of 3 mm/year (Ezer & Atkinson, 2014), meaning that future repetition of this study could produce differing results as tidally-driven inundation becomes more intense and widespread.

Conflict of Interest

The authors declare no conflicts of interest relevant to this study.

Data Availability Statement

All data and code are available on Dryad (Carr et al., 2024).

Acknowledgments
We thank David Bennett and Grant Caraway of the North Carolina Maritime Museum for access to their dock, and Dave Eggleston, Melissa LaCroce, and the NC State University Center for Marine Sciences and Technology for use of lab facilities. This work was supported by the U.S. National Science Foundation (NSF) award number 2047609 and the U.S. Geological Survey (USGS) Southeast Climate Adaptation Science Center award G23AC00548 via a Global Change Fellowship to M. Carr. This paper's contents are solely the responsibility of the authors and do not necessarily represent the views of the Southeast Climate Adaptation Science Center, USGS, or NSF.

References

Allen, T. R., Crawford, T., Montz, B., Whitehead, J., Lovelace, S., Hanks, A. D., et al. (2019). Linking water infrastructure, public health, and sea level rise: Integrated assessment of flood resilience in coastal cities. *Public Works Management & Policy*, *24*(1), 110–139. https://doi.org/10.1177/1087724X18798380

Befus, K. M., Kurnizki, A. P. D., Kroeger, K. D., Eagle, M. J., & Smith, T. P. (2023). Forecasting sea level rise-driven inundation in diked and tidally Restricted coastal lowlands. *Estuaries and Coasts*, *46*(5), 1157–1169. https://doi.org/10.1007/s12237-023-01174-1

Boehm, A. B. (2007). Enterococci concentrations in diverse coastal environments exhibit extreme variability. *Environmental Science & Technology*, *41*(24), 8227–8232. https://doi.org/10.1021/es071807v

Burkhart, T. H. (2013). *Biofilms as sources of fecal bacteria contamination in the stormwater drainage system in Singapore (Thesis)*. Massachusetts Institute of Technology. Retrieved from https://dspace.mit.edu/handle/1721.1/82805

Carr, M. M., Gold, A., Harris, A. R., Anarde, K., Hino, M., Sauers, N., et al. (2024). Fecal bacteria contamination of floodwaters and a coastal waterway from tidally-driven stormwater network inundation [Dataset]. *Dryad*. https://doi.org/10.5061/dryad.sxksn039s

Castrucci, L., & Tahvildari, N. (2018). Modeling the impacts of sea level rise on storm surge inundation in flood-prone urban areas of Hampton Roads, Virginia. *Marine Technology Society Journal*, *52*(2), 92–105. https://doi.org/10.4031/mtsj.52.2.11

Center for Operational Oceanographic Products and Services. (2022). *Tide & currents for Beaufort, Duke Marine Lab, NC-station ID: 8656483*. National Oceanic and Atmospheric Administration. Retrieved from https://tidesandcurrents.noaa.gov/stationhome.html?id=8656483

Converse, R. R., Piehler, M. F., & Noble, R. T. (2011). Contrasts in concentrations and loads of conventional and alternative indicators of fecal contamination in coastal stormwater. *Water Research*, *45*(16), 5229–5240. https://doi.org/10.1016/j.watres.2011.07.029

Dangendorf, S., Hendricks, N., Sun, Q., Klinck, J., Ezer, T., Frederikse, T., et al. (2023). Acceleration of US Southeast and Gulf coast sea-level rise amplified by internal climate variability. *Nature Communications*, *14*(1), 1–11. https://doi.org/10.1038/s41467-023-37649-9

Division of Water Resources. (2023). *2022 North Carolina 303(d) List*. North Carolina Department of Environmental Quality. Retrieved from https://edocs.deq.nc.gov/WaterResources/DocView.aspx?dbid=0&id=2738821

Ezer, T., & Atkinson, L. P. (2014). Accelerated flooding along the U.S. East coast: On the impact of sea-level rise, tides, storms, the Gulf stream, and the North Atlantic Oscillations. *Earth's Future*, *2*(8), 362–382. https://doi.org/10.1002/2014EF000252

Gallien, T. W., Sanders, B. F., & Flick, R. E. (2014). Urban coastal flood prediction: Integrating wave overtopping, flood defenses and drainage. *Coastal Engineering*, *91*, 18–28. https://doi.org/10.1016/j.coastaleng.2014.04.007

Gold, A., Anarde, K., Grimley, L., Neve, R., Srebnik, E. R., Thelen, T., et al. (2023). Data from the drain: A sensor framework that captures multiple drivers of chronic coastal floods. *Water Resources Research*, *59*(4), e2022WR032392. https://doi.org/10.1029/2022WR032392

Gold, A. C., Brown, C. M., Thompson, S. P., & Piehler, M. F. (2022). Inundation of stormwater infrastructure is common and increases risk of flooding in coastal urban areas along the US Atlantic coast. *Earth's Future*, *10*(3), e2021EF002139. https://doi.org/10.1029/2021EF002139

Gonzalez, R. A., Conn, K. E., Crosswell, J. R., & Noble, R. T. (2012). Application of empirical predictive modeling using conventional and alternative fecal indicator bacteria in eastern North Carolina waters. *Water Research*, *46*(18), 5871–5882. https://doi.org/10.1016/j.watres.2012.07.050

Habel, S., Fletcher, C. H., Anderson, T. R., & Thompson, P. R. (2020). Sea-level rise induced multi-mechanism flooding and contribution to urban infrastructure failure. *Scientific Reports*, *10*(1), 3796. https://doi.org/10.1038/s41598-020-60762-4

Hart, J. D., Blackwood, A. D., & Noble, R. T. (2020). Examining coastal dynamics and recreational water quality by quantifying multiple sewage specific markers in a North Carolina estuary. *Science of the Total Environment*, *747*, 141124. https://doi.org/10.1016/j.scitotenv.2020.141124

Health and Ecological Criteria Division, Office of Science and Technology. (2012). *Recreational water quality Criteria. (EPA-820-F-12-061)*. Environmental Protection Agency. Office of Water. Retrieved from https://www.epa.gov/sites/default/files/2015-10/documents/rwqc2012.pdf

IDEXX. (2019). *Standard test method for* Enterococci *in water using Enterolert. (ASTM D6503-19)*. IDEXX. Retrieved from https://www.astm.org/d6503-19.html

Koller, M. (2016). robustlmm: An R package for robust estimation of linear mixed-effects models. *Journal of Statistical Software*, *75*(6), 1–24. https://doi.org/10.18637/jss.v075.i06

Lewis, D. J., Atwill, E. R., Pereira, M., Das, G. C., & Bond, R. (2013). Spatial and temporal dynamics of fecal coliform and *Escherichia coli* associated with suspended solids and water within five northern California Estuaries. *Journal of Environmental Quality*, *42*(1), 229–238. https://doi.org/10.2134/jeq2011.0479

Lüdecke, D., Ben-Shachar, M., Patil, I., & Makowski, D. (2020). Extracting, computing and exploring the parameters of statistical models using R. *Journal of Open Source Software*, *5*(53), 2445. https://doi.org/10.21105/joss.02445

Lüdecke, D., Ben-Shachar, M. S., Patil, I., Waggoner, P., & Makowski, D. (2021). Performance: An R package for assessment, comparison and testing of statistical models. *Journal of Open Source Software*, *6*(60), 3139. https://doi.org/10.21105/joss.03139

Macías-Tapia, A., Mulholland, M. R., Selden, C. R., Loftis, J. D., & Bernhardt, P. W. (2021). Effects of tidal flooding on estuarine biogeochemistry: Quantifying flood-driven nitrogen inputs in an urban, lower Chesapeake Bay sub-tributary. *Water Research*, *201*, 117329. https://doi.org/10.1016/j.watres.2021.117329

Macías-Tapia, A., Mulholland, M. R., Selden, C. R., Loftis, J. D., & Bernhardt, P. W. (2023). Five years measuring the muck: Evaluating interannual variability of nutrient loads from tidal flooding. *Estuaries and Coasts*, *46*(7), 1756–1776. https://doi.org/10.1007/s12237-023-01245-3

Mallin, M. A., Williams, K. E., Esham, E. C., & Lowe, R. P. (2000). Effect of human development on bacteriological water quality in coastal watersheds. *Ecological Applications*, *10*(4), 1047–1056. https://doi.org/10.1890/1051-0761(2000)010[1047:EOHDOB]2.0.CO;2

McKenzie, T., Habel, S., & Dulai, H. (2021). Sea-level rise drives wastewater leakage to coastal waters and storm drains. *Limnology and Oceanography Letters*, *6*(3), 154–163. https://doi.org/10.1002/lol2.10186

National Oceanic and Atmospheric Administration. (2022). Northern hemisphere moon phases for 2022. Tides and currents—Astronomical data. Retrieved from https://tidesandcurrents.noaa.gov/moon_phases.shtml?year=2022

Olds, H. T., Corsi, S. R., Dila, D. K., Halmo, K. M., Bootsma, M. J., & McLellan, S. L. (2018). High levels of sewage contamination released from urban areas after storm events: A quantitative survey with sewage specific bacterial indicators. *PLoS Medicine*, *15*(7), e1002614. https://doi.org/10.1371/journal.pmed.1002614

Parker, J. K., McIntyre, D., & Noble, R. T. (2010). Characterizing fecal contamination in stormwater runoff in coastal North Carolina, USA. *Water Research*, *44*(14), 4186–4194. https://doi.org/10.1016/j.watres.2010.05.018

Price, M. T., Blackwood, A. D., & Noble, R. T. (2021). Integrating culture and molecular quantification of microbial contaminants into a predictive modeling framework in a low-lying, tidally-influenced coastal watershed. *Science of the Total Environment*, *792*, 148232. https://doi.org/10.1016/j.scitotenv.2021.148232

R Core Team. (2013). *R: A language and environment for statistical computing*. R Foundation for Statistical Computing. Retrieved from http://www.R-project.org/

R Core Team. (2022). *R: A language and environment for statistical computing*. R Foundation for Statistical Computing. Retrieved from https://www.R-project.org/

Sercu, B., Van De Werfhorst, L. C., Murray, J. L., & Holden, P. A. (2011). Sewage exfiltration as a source of storm drain contamination during dry weather in urban watersheds. *Environmental science & technology*, *45*(17), 7151–7157. https://doi.org/10.1021/es200981k

Shen, Y., Morsy, M. M., Huxley, C., Tahvildari, N., & Goodall, J. L. (2019). Flood risk assessment and increased resilience for coastal urban watersheds under the combined impact of storm tide and heavy rainfall. *Journal of Hydrology*, *579*, 124159. https://doi.org/10.1016/j.jhydrol.2019.124159

State Climate Office of North Carolina. (2022). Michael J Smith field Airport (KMRH) hourly and daily rainfall, June-August 2022 [Dataset]. *NOAA National Weather Service*. Retrieved from https://products.climate.ncsu.edu/data/

Strauss, B. H., Ziemlinski, R., Weiss, J. L., & Overpeck, J. T. (2012). Tidally adjusted estimates of topographic vulnerability to sea level rise and flooding for the contiguous United States. *Environmental Research Letters*, *7*(1), 014033. https://doi.org/10.1088/1748-9326/7/1/014033

Stumpf, C. H., Piehler, M. F., Thompson, S., & Noble, R. T. (2010). Loading of fecal indicator bacteria in North Carolina tidal creek headwaters: Hydrographic patterns and terrestrial runoff relationships. *Water Research*, *44*(16), 4704–4715. https://doi.org/10.1016/j.watres.2010.07.004

Sweet, W., Hamlington, B. D., Kopp, R. E., & Zuzak, C. (2022). *Global and regional sea level rise scenarios for the United States: Updated mean projections and extreme water level probabilities along U.S. Coastlines (technical report)* (p. 111). National Oceanic and Atmospheric Administration. Retrieved from https://aambpublicoceanservice.blob.core.windows.net/oceanserviceprod/hazards/sealevelrise/noaa-nos-techrpt01-global-regional-SLR-scenarios-US.pdf

Wade, T. J., Pai, N., Joseph, N., Eisenberg, S., & Colford, J. M. (2003). Do U.S. Environmental protection agency water quality guidelines for recreational waters prevent gastrointestinal illness? A systematic review and meta-analysis. *Environmental Health Perspectives*, *111*(8), 1102–1109. https://doi.org/10.1289/ehp.6241